A Trans Acting Ribozyme that Phosphorylates Exogenous RNA †

3 **AUTHORS**, INCLUDING:

David G Nickens

Indiana University Bloomington

16 PUBLICATIONS   **226** CITATIONS

SEE PROFILE

Donald H Burke

University of Missouri

63 PUBLICATIONS   **1,551** CITATIONS

SEE PROFILE

A Trans Acting Ribozyme that Phosphorylates Exogenous RNA[†]

Dayal Saran,[‡] David G. Nickens, and Donald H. Burke*,[‡]

Department of Chemistry, Indiana University, 800 East Kirkwood Avenue, Bloomington, Indiana 47405

Received June 7, 2005; Revised Manuscript Received August 30, 2005

ABSTRACT: The structural complexity required for substrate recognition within an active site constrains the evolution of novel catalytic functions. To evaluate those constraints within populations of incipient ribozymes, we performed a selection for kinase ribozymes under conditions that allowed competition for phosphorylation at nine candidate sites. Two candidate sites are the hydroxyl groups on a "quasi-diffusible" chloramphenicol (Cam) moiety tethered to the evolving library through an inert, flexible linker. A subtractive step was included to allow only seven ribose 2′ hydroxyls to compete with the two Cam hydroxyls for phosphorylation. After the library was incubated with gamma-thio-ATP (ATPγS), active species were recovered from a polyacrylamide gel containing [(*N*-acryloylamino)phenyl] mercury (APM) and amplified for further cycles of selection. Activity assays on selected isolates and truncated derivatives identified the essential secondary structure of the dominant RNA motif. Phosphorylation was independent of the Cam moiety, indicating ribose 2′ phosphorylation. The dominant motif was separated into catalytic "ribozyme" and "substrate" strands. Partial alkaline digestion of the substrate strand before and after phosphorylation identified the precise modification site as the first purine (R) within the required sequence 5′-RAAAANCG-3′. The reaction shows approximately 10-fold preference for ATPγS over ATP and is independent of pH over a wide range (5.5−8.9), consistent with a dissociative reaction mechanism that is rate-limited by formation of a metaphosphate transition state. Divalent metal ions are required, with a slight preference of $Mn^{2+} > Mg^{2+} > Ca^{2+}$. Lack of reactivity in $[Co(NH_3)_6]^{3+}$ indicates a requirement for inner sphere contact with the metal ion, either for structural stabilization, catalysis, or both.

In vitro selection, or systematic evolution of ligands by exponential enrichment (SELEX),[1] identifies functional nucleic acids with novel activity from highly complex libraries of random nucleic acid sequences. The "RNA world" hypothesis postulates a primitive RNA-directed metabolism before the evolution of genetically encoded protein synthesis. This hypothesis has received support from the identification of RNA molecules that catalyze a variety of chemical transformations, including phosphodiester bond formation (*1*), limited RNA polymerization (*2*), self-aminoacylation (*3*), amide bond formation (*4*), carbon−carbon bond formation (*5*), self-alkylation (*6*), acyl transfer (*7*), glycosidic bond cleavage (*8*), and polynucleotide phosphorylation (*9*) (reviewed by Burke (*10*)).

Phosphoryl group transfer is one of the most ubiquitous reactions in small molecule and protein metabolism, with prominent roles in biosynthesis and catabolic reactions and in the regulation of enzyme activity, quaternary assembly, and gene expression. The reaction is therefore of fundamental biological significance. RNA-catalyzed phosphorylations are attractive to study for several reasons. First, the chemical mechanisms of many natural kinases have been studied extensively, facilitating comparison of ribozyme catalysis and protein catalysis of equivalent reactions. Second, the underlying chemistry of phosphorylation reactions is relatively simple and can be easily examined using radioactive or thiolated phosphoryl donors. In addition, novel kinase ribozymes can be developed as highly valuable tools for engineering artificial gene regulation and metabolism.

Ribozymes that catalyze phosphoryl transfer were first selected by Lorsch and Szostak by incubating a random-sequence RNA library with ATPγS. Species that transferred the γ-thiophosphoryl group onto themselves became tagged with a sulfur and were recovered via formation of a disulfide bond with a solid support (*9*). Curtis and Bartel (personal communication) used a similar strategy to recover self-phosphorylating ribozymes from a library of mutated variants of another ribozyme with an entirely different function (aminoacyltransfer). Self-kinasing nucleic acid catalysts composed entirely of DNA (DNAzyme) have also been selected. When Li and Breaker incubated a ssDNA library with a mixture of all four NTPs or all four dNTPs, only the molecules that acquired a 5′ phosphate became substrates for ligation to an oligonucleotide tag, which then served as a primer binding site for PCR amplification (*11*). Both the Szostak and the Breaker groups produced nucleic acid catalysts that phosphorylated their own 5′ ends. In both cases,

FIGURE 1: Selection process: (A) Cam-linked oligo ligated to the RNA pool. (B) Hybrid RNA pool construct. Lowercase letters correspond to ribonucleotides from 5′ and 3′ primer binding region, and uppercase letters correspond to deoxynucleotides of Cam linked DNA oligo ligated to the RNA. Location of the 10−23 DNAzyme cleavage site is indicated by the solid wedge. (C) Selection progress. Column 11* and 12* are the percentages of the purified, self-phosphorylated RNA that passed through the APM layer after 10−23 cleavage during the subtractive selection step. (D) Subtractive selection scheme. Details are described in the text. Asterisk (*) indicates the APM layer in a trilayer acrylamide gel.

the 5′ OH phosphoryl acceptors were held in the enzyme active sites through Watson−Crick base pairing between the adjoining nucleotides and an internal guide sequence within the (deoxy)ribozyme. An engineered version of one of the ribozymes (Kin.46) can also phosphorylate the 5′ end of a six- or seven-nucleotide oligo complementary to the internal guiding sequence of the ribozyme (9).

Some of the kinase ribozymes can self-phosphorylate at internal 2′ positions (9), although neither natural protein enzymes nor engineered nucleic acid enzymes have been described that act in trans to phosphorylate the 2′ position of exogenous RNA substrates. The rare natural examples of RNAs that possess 2′ phosphates are not generated through phosphoryl transfer but are instead intermediates of splicing reactions. For example, both pre tRNA[leu3] (yeast) (12) and the cyclized version of RNA fragment Ω73 (tobacco mosaic virus) (13, 14) are formed via the ligation of the 2′-3′ cyclic phosphate of an upstream fragment with the 5′ monophosphate of a downstream fragment. This reaction leaves a phosphate on the 2′ hydroxyl that is subsequently removed by phosphatases. Sekine and co-workers developed a chemical scheme for the synthesis of 2′ phosphorylated and thiophosphorylated oligonucleotides and studied the thermodynamic and conformational properties of RNA and DNA molecules containing those modifications (15, 16). Molecular dynamics simulations and T_m measurements on singly phosphorylated RNA and DNA duplexes demonstrated that the 2′ phosphorylated ribose moiety predominantly preferred C2′-endo over C3′-endo conformation. Because the sugars in B-form DNA are predominately C2′-endo, while those of A-form RNA are predominately C3′-endo, the 2′ phosphorylation strongly destabilized RNA duplexes without significantly affecting the stability of DNA duplexes (16).

In the present work, we describe a new ribozyme that phosphorylates a specific internal 2′ hydroxyl of an exog-

enous RNA containing an unpaired 5′RAAAANCG3′ sequence where R (any purine) is the site of phosphorylation. This is the first demonstration of a *trans*-acting ribozyme that phosphorylates the 2′-OH of an exogenous substrate. This ribozyme was created by first selecting RNA molecules that phosphorylate 2′ hydroxyls in a specific region, then removing extraneous peripheral sequences. Interestingly, internal 2′ phosphorylation arose despite the availability of an alternative small molecule substrate tethered to the RNA library. These new ribozymes shed light on the evolution of catalytic function, and they could be engineered to phosphorylate intracellular biological RNA targets.

MATERIALS AND METHODS

Materials. All the oligos were purchased from Integrated DNA technologies (IDT). ATPγS was purchased from Sigma, and γ[32]P-ATP was purchased from MP Biomedicals. Ligase enzyme was purchased from Epicenter. Chloramphenicol (Cam) linked 8-mer DNA oligo (Figure 1A) was synthesized by condensing the Cam base with a 5′ amino-modified 8-mer DNA (NH$_2$−triethylene glycol−GGAC-CCTA-3′) with bifunctional linker disuccinimidyl glutarate (DSG, purchased from Pierce) (DS and DHB, in preparation). MALDI-TOF mass spectroscopic analysis of the purified CAM-linked 8-mer DNA oligo yielded a single peak at 3096.57 mass units, which is very close to the expected value of 3095 mass units.

Selection Scheme. The initial RNA library was generated by transcribing a double-stranded DNA library created from Klenow extension and PCR amplification of approximately 10[14] different single-stranded DNA sequences purchased from Operon (Alameda, CA). The hybrid RNA pool for the in vitro selection was synthesized by ligating the Cam-linked 8-mer DNA oligo to the RNA library. The organization of the final pool is shown in Figure 1B. Ligation was performed

by incubating RNA (1 μM) with 8-mer DNA oligo (1.5 μM) and 24-mer DNA bridge (3 μM) in a buffer that contained 1 mM ATP and T4 DNA ligase at 37 °C for 5 h. The sequence of the DNA bridge (5′-GATTCGCTTTTCCCTA-GGGTCC-3′) is complementary to both the 8-mer DNA oligo and to the 5′ PBS of the RNA. The first round of in vitro selection was performed by heating 6 nmol of hybrid pool in metal-free buffer to 82 °C for 2 min and gradually cooling to 50 °C in 5 min. To this solution was added monovalent ions to the final concentration of 50 mM K$^+$, 150 mM Na$^+$ in 50 mM PIPES buffer at pH 6.5. This solution was cooled from 50 to 37 °C gradually in 5 min. To this solution was added divalent ions to the final concentration of 20 mM Mg^{2+}, 5 mM Ca^{2+}, 2.5 mM Mn^{2+}, 10 μM each for Co^{2+}, Cu^{2+}, Zn^{2+}, and Ni^{2+}. The phosphorylation reaction was initiated by adding ATPγS to a final concentration of 5 mM. After the reaction mixture was incubated at 37 °C for 14 h, RNA was precipitated by adding two volumes of ethanol. The pellet was washed gently with 70% ethanol, resuspended in H$_2$O, and precipitated again to remove extra ATPγS. To recover thiophosphorylated product, the RNA was run for 2 h at 30 V/cm on a three-layered 8% denaturing polyacrylamide gel with an APM (acryloyl-aminophenylmercuric chloride) layer in the middle. The region at the interface of the upper non-APM and APM layers, where active RNAs were immobilized, was cut from the gel. RNA was recovered by crushing the gel slice in the presence of 50 mM dithiothreitol to disrupt the mercury sulfur interaction. The gel slurry was filtered through 0.22 μm cellulose acetate membrane filters, and RNA in the filtrate was ethanol precipitated as above. Purified RNAs were RT-PCR amplified for use in the next round of selection. A total of 1 nmol of RNA was used in the second round of selection, and 500 pmol of RNA was used in subsequent rounds of selection.

Subtractive Selection. 1 μM thiophosphorylated RNA was incubated with the 10−23 DNAzyme (*19*) 5′-GTATGAT-TCGGGCTAGCTACAACGATTTTCCCTAG-3′ (10 μM) at 37 °C overnight in the presence of 50 mM Tris-HCl at pH 7.5 and 20 mM MgCl$_2$. The reaction mixture was separated on a three-layered APM gel as discussed above. This time RNA that migrated through the APM next to a 110 nucleotide size marker was purified and amplified for the next round of selection (Figure 1D).

Activity Assay on Substrate/Ribozyme Complex. DNA−RNA−DNA substrate strands were synthesized by Integrated DNA Technologies. Ribozyme assays were performed under conditions similar to those used in the selection except as noted in the text. The 2PTmin3.2 ribozyme strand (5 μM) and 5′ radiolabeled substrate strand (1 μM) were annealed as described above. The percentage of the substrate that became phosphorylated when γ^{32}P-ATP was used as the phosphate donor was calculated by measuring the radioactivity incorporated into the substrate band and normalizing to the signal generated by equimolar substrate labeled by polynucleotide kinase using the same batch of γ^{32}P-ATP as that used in the ribozyme-catalyzed reaction. Kinetic rate constants (k_{obs}) of the fraction of substrate phosphorylated at time t (F_t) in the presence of 30 mM single metal ions were calculated using a single-exponential first-order rate equation [$F_t = F_\infty(1 - e^{-kt})$], where F_∞ is the fraction phosphorylated at infinite time.

RESULTS

Selection of Novel Thiophosphoryl Transferase Ribozymes. The library used in the selection of novel kinase ribozymes contained approximately 10^{14} unique species, each with 70 randomized positions. Each 118 nt RNA transcript was enzymatically ligated to a chloramphenicol (Cam)-modified 8-mer DNA oligonucleotide (Figure 1A). The library was incubated for 14 h with 5 mM ATPγS to provide an opportunity for ribozyme-catalyzed thiophosphoryl transfer. Potential phosphoryl acceptors at this stage include the two hydroxyls of Cam, the 118 2′ OH of the transcript, and the terminal 3′OH. The reaction products were separated on a trilayer polyacrylamide gel (*17*) in which the middle layer was doped with *N*-acryloylamino-phenyl-mercuric chloride (APM) (*18*). Catalytically active RNA species that acquired a thiophosphoryl group were retained at the APM interface due to the strong coordinate bond between sulfur and mercury, whereas the unaltered species pass through. RNA was recovered from the excised APM interface, RT/PCR amplified, and transcribed for the next round of selection. Product accumulation above background was first detected in the ninth round of selection and climbed to approximately 40% during the eleventh round of selection (Figure 1B).

Because the pK_a of the Cam hydroxyls (10.2) is similar to that of a ribose 2′ hydroxyl (10.4), intrinsic reactivity is likely to be similar at the two classes of sites. To permit competition between phosphorylation of the tethered substrate and phosphorylation of the internal 2′OH, the self-phosphorylated molecules recovered from the APM interface during selection cycles 11 and 12 were subjected to a subtractive procedure that removed most internally phosphorylating species. Specifically, the recovered RNAs were incubated with a DNAzyme of the "10-23" family (*19*) that directs cleavage after ribonucleotide G8 in the primer binding region of the RNA. When the cleaved products were loaded onto a second APM gel, the two fragments partitioned according to the location of the thiophosphoryl group acquired during the incubation with ATPγS. Those ribozymes that had acquired a thiophosphoryl group on Cam or on one of the first seven ribonucleotides passed through the APM layer, while those that had been thiphophorylated downstream of the cleavage site were again retained at the APM interface (Figure 1C). This strategy therefore establishes a competition between the two sterically accessible Cam hydroxyls and the seven ribose 2′ hydroxyls that lie upstream of the DNAzyme cleavage site. Although nucleotide G8 is also removed by the 10−23 cleavage, phosphorylation of its ribose hydroxyl would have blocked cleavage by the DNAzyme, and it is therefore not considered. The non-thiophosphorylated RNAs were recovered and RT/PCR amplified. After the two selection cycles that included this subtractive step, approximately 75% of the product RNA passed through the APM layer and is thus assumed to label 5′ to the 10−23 DNAzyme cleavage site. This material was cloned for sequencing and analysis.

Initial Screens of the Selected Population. Nucleotide sequences from 24 independent isolates fell into seven related families, two of which had single representatives. Five families carried a consensus motif of 5′-UGCGAACUA-3′ at the 3′ end of the original 70N random region and partial matches to this motif are present near the 3′ends of the other
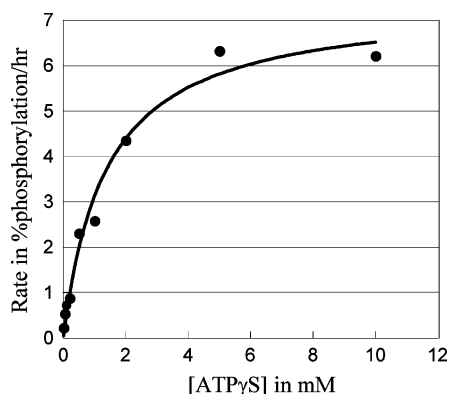
FIGURE 2: Michaelis-Menten kinetics for self-thiophosphorylation. Rates were calculated from slopes of linear fits to the initial time points at different concentrations of ATPγS.

two families (Supporting Information Figure 1). Catalytic activity was monitored for transcripts generated from 11 of the cloned isolates representing one or two members from each sequence family. First, to determine whether the selected ribozymes required the sulfur of the ATPγS, nonradiolabeled RNA was ligated to the Cam-modified 8-mer DNA oligo, and the Cam-DNA/RNA hybrids were incubated for 14 h with $[\gamma\text{-}^{32}P]$ ATP. Each isolate became radiolabeled, demonstrating that they catalyze phosphoryl transfer in addition to thiophosphoryl transfer. When the radiolabeled products were purified and cleaved with the 10−23 DNAzyme, the label was retained on the 5′ cleavage fragment, demonstrating that the subtractive step of the selection had succeeded in limiting regiospecificity to this portion of the molecule (Supporting Information Figure 2A). When auto-thiophosphorylated transcripts were recovered from APM gels and reverse transcribed with a 5′ radiolabeled DNA primer, a single modification-dependent pause site was evident near the 5′ end of the primer binding sequence. The reverse transcription product is slightly smaller than the 118 nt DNA marker, suggesting that the modification site might lie within the RNA portion between positions +1 and +7 (GG-GAAAA) (Supporting Information Figure 2B).

Transcribing the entire 126 nucleotide DNA−RNA hybrid as a single RNA molecule yields a transcript in which the deoxynucleotides in positions −8 to −1 are replaced with ribonucleotides and the tethered Cam is missing. Even with these changes the simplified, all-RNA transcripts reacted to an equivalent extent as the hybrid Cam-DNA/RNA species. The same isolates were catalytically inactive when transcribed as 118 nt transcripts initiated from the +1 position. Positions −8 to −1 are therefore required components of the active structure. When transcribed as 126-nt RNAs, each of these 11 isolates (including members of families three and seven) gave similar auto-thio phosphorylation rates of 0.07 to 0.10 h^{-1} when the reactions were carried out in 5 mM ATPγS. The concentration dependence of the reaction reveals saturable binding of the substrate consistent with Michaelis−Menten-type kinetics. The kinetic profile of isolate 2PT3.2, which is typical of the 11 isolates examined, yielded k_{cat} and $K_m^{ATP\gamma S}$ values of 0.074 ± 0.004 h^{-1} and 1.3 ± 0.2 mM, respectively (Figure 2).

A Simplified, Trans-Acting Ribozyme. The sequences of all of the isolates were predicted by mfold (http://www.bioinfo.rpi.edu/applications/mfold/old/rna/) to fold into a

common secondary structure (Figure 3A). A ribozyme with only this shared structural core (75 nt) catalyzed its thiophosphorylation with a rate that was equivalent to that of the full-length transcript (Figure 3B). Deleting the internal loop within the 3′ PBS further simplified the ribozyme (57 nt) and increased activity to nearly double that of the full-length transcript (Figure 3C). Finally, separating the "left" and "right" sides of the ribozyme generated a two-stranded ribozyme/substrate complex that catalyzed thiophosphorylation of the substrate strand as rapidly as the fastest *cis*-acting ribozyme (Figure 3D). This *trans*-acting configuration, denoted 2PTmin3.2, proved to be convenient for further analysis of the catalytic reaction.

Dissecting the Functional Core of Isolate 2PTmin3.2. Mutations and deletions were introduced at specific positions to ascertain the sequence requirements for the substrate. Single-turnover thiophosphoryl transfer activity was measured for a substrate in which all of the ribonucleotides except for the six in loop 1 were replaced with deoxyribonucleotides. The resulting DNA−RNA−DNA substrate reacted with equivalent rate and yield as the all-RNA substrate, confirming that the modification site lies within the GGAAAA segment and demonstrating that none of the other positions is required to carry a ribose sugar. No thiophosphoryl transfer was evident for complexes that utilized all-DNA versions of the ribozyme or substrate strand. Subsequent mutational studies therefore utilized 5′ radiolabeled DNA−RNA−DNA substrates and all-RNA ribozymes (Figure 3E). Nucleotide positions of this complex are identified by position number and by the letter "R" for the ribozyme strand or "S" for substrate strand. Stems and bulges are numbered according to their sequential order of appearance in the substrate strand.

Two mutations examined the role of the predicted pair between U14$_R$ and G15$_S$. First, a ribozyme carrying a U14$_R$C mutation, which replaces the G·U pair with a more stable G·C pair, phosphorylated the substrate poorly (Figure 4, column B), ruling out a model in which this pair provides generic structural stabilization. The potential G·U pair was then disrupted by a G15$_S$T mutation. The substrate carrying this replacement was phosphorylated at least as well as the parental substrate strand (Figure 4, column C). Therefore, although the G·U pair is predicted by mfold to base pair, these nucleotides are shown as being unpaired in Figure 3E.

Bulge 2 is predicted to form in only a subset of the isolates, and its sequence is not conserved. Simultaneously substituting A18$_S$G and A19$_S$G had no significant effect on thiophosphoryl transfer (Figure 4, column D). Next, nucleotides in either the ribozyme strand (GUAA → UU) or substrate strand (AA → TTAC) were changed to convert the bulge into a continuous stem. Both constructs were active, although the product yield was approximately one-third the yield obtained by 2PTmin3.2 (Figure 4, columns E and F). Thus, while the specific sequence of bulge 2 is not required, its presence enhances ribozyme reactivity. Several stem 2 mutations were introduced to ascertain the significance of the CG pairs. These positions are conserved in the ribozyme strand among several sequence families; however, the base pairing partners in the substrate strand were originally part of the 5′ PBS and therefore could not yield conservation data. Disruption of stem 2 by simultaneously introducing C16$_S$G and G17$_S$C mutations in the substrate strand (Figure 4, column G) eliminated activity. This construct effectively
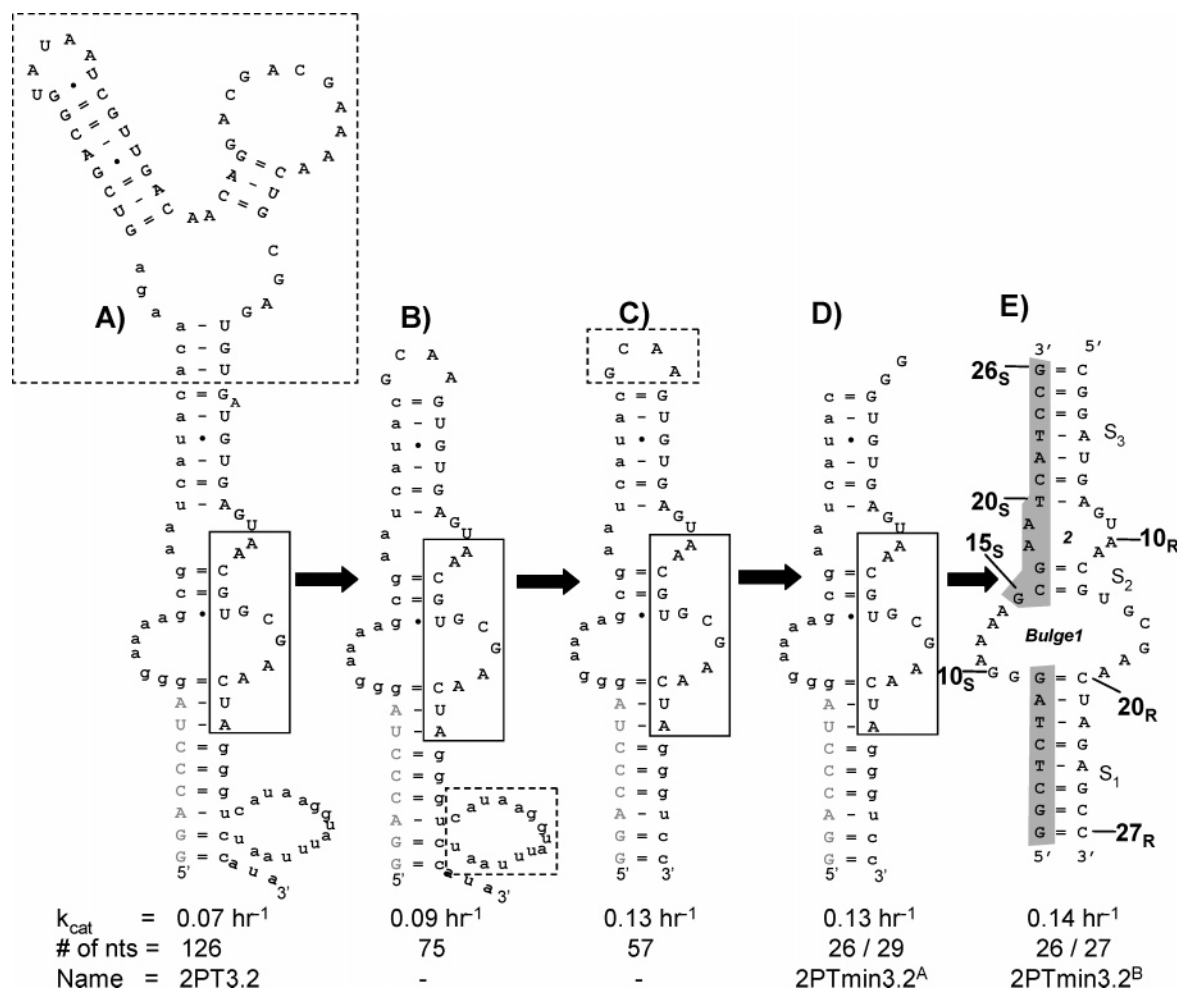
FIGURE 3: Minimization of ribozyme: (A) Secondary structure of the full 126-mer 2PT3.2. (B−D) Sequential minimization of 2PT3.2 by keeping only the core region shared by all the recovered isolates. Grey letters represent positions that were deoxyribonucleotides in the initial selection. Sequence in the solid box is conserved in most of the isolates. Primer binding regions are represented by lowercase letters. Nucleotides in the dotted box indicate segments that were deleted in the subsequent structure. (E) Grey shaded nucleotides were deoxynucleotides in this construct. Nucleotides of substrate and ribozyme strands are denoted by its position and by the letters "S" and "R". Stems and bulges are numbered according to their sequential order of appearance in the substrate strand. Rate constants, number of nucleotides, and names of individual species are given across the bottom. The minor sequence differences between ribozymes 2PTmin3.2^A (panel D) and 2PTmin3.2^B (panel E) were introduced to strengthen stems 1 and 3.
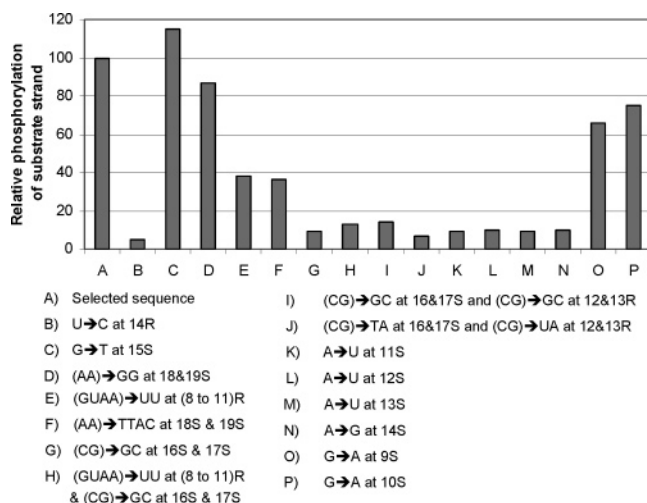
FIGURE 4: Mutational analysis. All activities are plotted relative to the activity of the construct shown in Figure 3E. Columns A−P correspond to mutations described below the graph.

fused bulges 1 and 2. To restore some structural stability to this region, the same two mutations were assessed in the

context of a ribozyme strand that zippered together the nucleotides in bulge 2 (the GUAA → UU mutation above). This construct, which is characterized by an expanded bulge 1, was also inactive (Figure 4, column H). Finally, alternative pairings were introduced into stem 2 by inverting the two base pairs (Figure 4, column I) or by replacing them with UA:UA pairs (Figure 4, column J). Both combinations showed greatly reduced activity relative to 2PTmin3.2. Thus, while it is likely that the CG nucleotides in positions 16_S and 17_S pair with the CG nucleotides in positions 12_R and 13_R to form stem 2, these positions do not tolerate substitution to other nucleotides.

To determine sequence specificity in the substrate strand, mutations were introduced at each position of bulge 1 within the substrate strand. Positions 11_S to 13_S were mutated individually to U. To avoid introducing cross-strand base pairing, positions 9_S and 10_S were mutated to A rather than to U and position 14_S was mutated to G. Catalytic activity was abolished or severely curtailed by mutations $A11_SU$, $A12_SU$, $A13_SU$, and $A14_SG$ when these were introduced individually (Figure 4, columns K−N). In contrast, positions
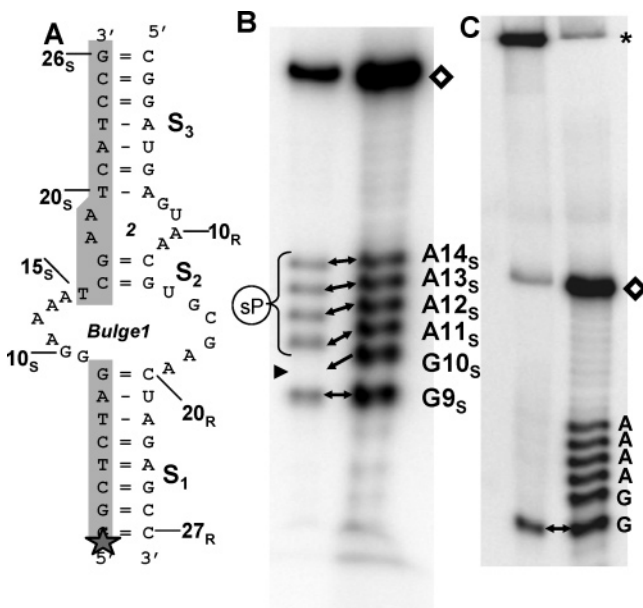
FIGURE 5: Precise mapping of thiophosphorylation site. (A) A ribozyme/substrate complex is used in the assay. Boxed nucleotides are deoxynucleotides. Star represents the radiolabel. (B) Partial alkaline digestion of thiophosphorylated (lane 1) and unphosphorylated (lane 2) substrate strands indicate the phosphorylation site to be the $G10_S$ position. Triangle shows the position of the missing band. Full-length substrate strand is indicated by ◊. (C) Same samples as in panel B were loaded onto gel containing an APM layer (asterisk).

9_S and 10_S each tolerated G → A substitutions (Figure 4, columns O and P). These data therefore suggest a tolerence for A or G at positions 9 and 10, an absolute requirement for adenosines at positions 11_S to 14_S, and an absolute requirement for C and G at positions 16_S and 17_S respectively.

Precise Mapping of the Reactive Hydroxyl. Two complementary approaches mapped precisely the site that is thiophosphorylated by ribozyme 2PTmin3.2. Both approaches utilized 5′ radiolabeled DNA−RNA−DNA substrate that had been thiophosphorylated by 2PTmin3.2 (Figure 3E) and purified by mercury gel electrophoresis. This product was partially degraded under alkaline conditions to generate a ladder of digestion products with cleavage sites at each ribose hydroxyl. In the first approach, the alkaline digestion ladder was separated on a normal polyacrylamide gel. The product of alkaline cleavage at $G9_S$ comigrated with the corresponding product from native substrate (Figure 5B).

However, the product of alkaline cleavage at position $G10_S$ is missing, and higher molecular weight cleavage products are all shifted downward. These data are consistent with thiophosphorylation of the 2′OH of $G10_S$ in that this modification would prevent nucleophilic attack by the 2′ oxygen of $G10_S$ on the adjacent phosphate, and all cleavage products on the 3′ side of this site would carry additional negative charge due to the appended phosphate. In the second approach, partially digested substrate was loaded onto the APM trilayered gel. The product of alkaline cleavage at $G9_S$ passed through the APM layer and again comigrated with the corresponding nonthiophosphorylated species. However, all higher molecular weight cleavage products were retained in the APM layer, indicating that they that contained a thiophosphate (Figure 5C). These data firmly establish the 2′ OH of $G10_S$ as the phosphorylation target.
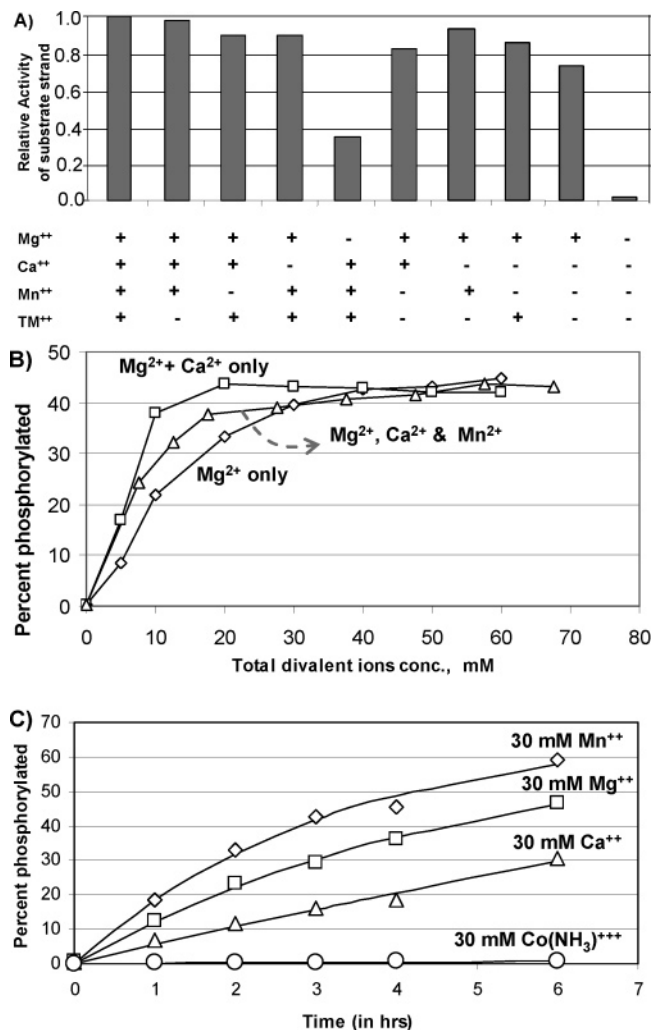

FIGURE 6: Metal dependence of thiophosphorylation reaction. (A) Ribozyme-catalyzed thiophosphorylation yields after incubation for 11 h in the presence of different combinations of metal ions are plotted relative to the yields obtained in the original selection buffer. TM^{2+} represents transition metals. (B) Product accumulation after 11 h is plotted as a function of total metal ions concentration using the composition indicated here and in the text. (C) Time course of product accumulation in the presence of 30 mM Mn^{2+} (diamonds), 30 mM Mg^{2+} (squares), 30 mM Ca^{2+} (triangles), and 30 nM Co-$(NH_3)_6^{3+}$ (circles).

Metal Ion Dependence. Metal ions can powerfully influence the outcome of a selection. For example, previous ribozyme selections carried out in the presence of Ni^{2+} or Cu^{2+} yielded nucleic acid species that absolutely required these divalent metal ions (*4, 20*). The present work included a number of alkaline earth and transition metal ions to present the evolving library with the opportunity to exploit the unique chemical reactivity of each. To determine which components of the selection buffer are utilized by 2PTmin3.2, thiophosphoryl transfer reaction rates under various ionic conditions were plotted relative to the rate observed under the conditions of the selection (Figure 6A). The ribozyme rate is unaffected or only slightly reduced by the omission of Mn^{2+}, Ca^{2+}, the trace transition metals, or combinations of these. Approximately one-third maximal yield was obtained when Mn^{2+} (2.5 mM), Ca^{2+} (5 mM), and transition metals were supplied as the only divalent ions.

These results could reflect either a preference for Mg^{2+} or a general requirement for high concentrations of divalent

metal ions. To address this question, product accumulation was monitored using one of three mixtures of divalent metal ions. In the first set of reactions, Mg^{2+} was supplied as the only divalent metal ion. Product formation increased with increasing concentration of Mg^{2+}, reaching a plateau by around 30 mM $MgCl_2$ and half-maximal yield at 10 mM $MgCl_2$. The second set of reactions were carried out identically to the first set, except that each reaction also contained 5 mM Ca^{2+} and 2.5 mM Mn^{2+}. When product accumulation was plotted as a function of total divalent ion concentration, yield increased faster than when Mg^{2+} was the only divalent ion present. In the third set of reactions, Mn^{2+} and Ca^{2+} were the only divalent ions included in the reaction and were kept in equimolar concentrations. This titration gave the fastest approach to saturation, reaching a plateau between 10 and 20 mM total divalent ion and half-maximal yield by approximately 6 mM divalent ion (Figure 6B).

The data above show that ribozyme activity depends strongly on total divalent ion concentration and to a lesser degree on the identity of the divalent metal ions available. Product accumulation was therefore monitored for single-turnover reactions in which metal ion concentration was held constant at 30 mM and only one metal ion at a time was included in the reaction. Product accumulation was fastest for reactions containing 30 mM Mn^{2+}. These data fit well to a single-exponential kinetic function, giving an observed rate constant (k_{obs}) of 0.31 hr^{-1}. Reactions with 30 mM Mg^{2+} or with 30 mM Ca^{2+} gave progressively less product and slower k_{obs} (0.21 and 0.045 h^{-1}) (Figure 6C). These small differences in the rates could be due to subtle variations in the size, shape, or charge density of these three metal ions, to differences in propensity to form inner-sphere contacts (coordinate-covalent metal−oxygen or metal-sulfur bonds), or to other properties of the metal ions. Notably, the observed rate constants calculated from the fit to the exponential function (k_{obs}) are approximately 2-fold higher than the rate constants calculated by fitting the initial time points to a straight line. The exponential fit takes into account the fact that less than 100% of the substrate is converted into product and thus more accurately represents the underlying kinetics process.

To determine whether the metal ions are enhancing the reaction due to formation of the inner sphere contact with the RNA, the self-labeling reaction was carried out in the presence of $Co(NH_3)_6^{3+}$. The Co−N bonds exchange very slowly under the conditions of these assays, essentially preventing metal−RNA interactions. No reactivity was observed in the presence of $Co(NH_3)_6^{3+}$, suggesting that inner sphere metal ion contacts may be essential for the catalytic reaction (Figure 6C).

Evidence for S_N1-like (Dissociative) Reaction Mechanism. Phosphoryl transfers can take place through reaction mechanisms that are primarily associative (S_N2-like), primarily dissociative (S_N1-like), or a blend of the two. In a purely associative reaction, a complete covalent bond is formed between the acceptor and the phosphorus prior to breaking the phosphorus−donor bond. The rate-determining step can thus be activation of the phosphoryl acceptor. For example, the intrinsic nucleophilicity of a ribose 2′ oxygen is increased 100-fold upon deprotonation from a hydroxyl to an oxyanion (*21*). Predominately associative reactions often show strong
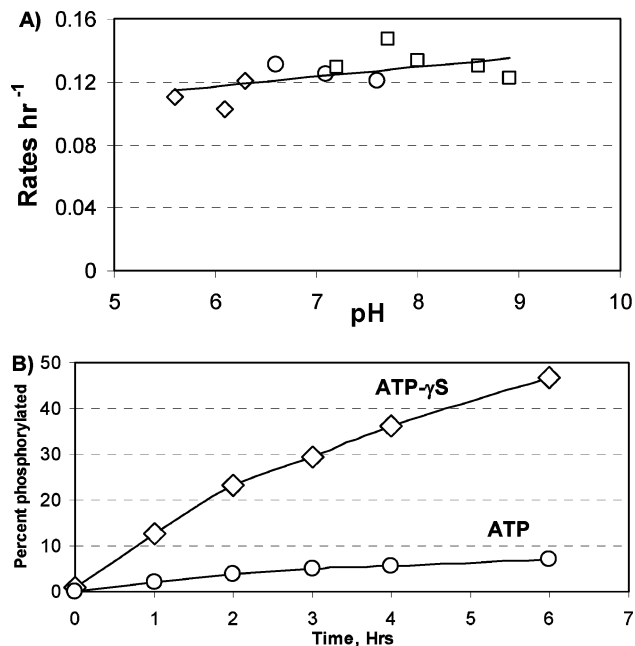

FIGURE 7: Evidence for dissociative reaction mechanism. (A) Initial rates of thiophosphorylation by ribozyme 2PTmin3.2 were measured using the same buffer composition as that used during the selection except that the pH buffer was 50 mM MES (diamond) at pH 5.6, 6.1, 6.3, PIPES (circles) at pH 6.6, 7.1, 7.6, and TRIS (squares) at pH 7.2, 7.7, 8.0, 8.6, 8.9. Rates at different pH values were calculated using the slope of initial time points. (B) Phosphoryl donor specificity. 10-fold difference in the rates was monitored using 5 mM ATPγS (diamonds, 0.13 h^{-1}) vs 5 mM ATP (circles, 0.015 h^{-1}) as phosphate donor.

pH dependence similar to the log−linear relationship between the rate of hammerhead ribozyme-catalyzed strand cleavage and pH. In a purely dissociative reaction, the rate-determining step is the dissociation of the phosphorus from the donor oxygen to form a more electropositive metaphosphate intermediate. This is followed by fast attack of a nucleophile on the electrophilic phosphorus to form the new acceptor−phosphorus bond. Reactions that go through a metaphosphate intermediate in solution yield racemic mixtures of products, while enzyme-catalyzed reactions are stereochemically controlled. Furthermore, Jencks and Cleland have each separately shown that most enzyme-catalyzed dissociative reactions probably go through metaphosphate-like transition states rather than metaphosphate intermediates (*22−24*). To the extent that dissociation of the donor−phosphorus bond is rate-determining, the observed reaction rate is independent of the protonation state of the acceptor nucleophile, making purely S_N1 type reactions essentially independent of the pH. Most phosphoryl transfers occur concertedly as a blend of the two archetypal mechanisms, fueling extensive debate over the degree of covalent character of the transition states (*25−28*).

When single-turnover thiophosphoryl transfer rates were measured for 2PTmin3.2, the rate remained virtually unchanged over the range from pH 5.6 to pH 8.9 (Figure 7A). While this would seem to suggest a dissociative reaction mechanism, the flat pH−rate profile could potentially mask the effects of an acid/base pair responsible for deprotonating the nucleophile and protonating the leaving group, as the effects of pH on one of these two species could cancel out the effect of the other and produce the flat pH−rate profile. We consider this to be unlikely, since ADP is a very good

leaving group that is unlikely to require protonation, and hence there is unlikely to be a requirement for general acid catalysis.

A primary determinant of dissociative phosphoryl transfers is the stability of the metaphosphate-like transition state (*22*). The presence of the polarizable sulfur in ATPγS is expected to stabilize the transition state by contributing electron density to the developing positive charge on the phosphorus. The sulfur in thiometaphosphate makes it more stable than metaphosphate because accumulation of negative charge on the nonbridging ligands (oxygens and sulfur) is made more facile with the more easily polarized sulfur than with oxygen. These effects predict faster reactivity with ATPγS than with ATP. Therefore, the rate of thiophosphorylation using ATPγS as donor was compared with the rate of phosphorylation using γ^{32}P-ATP as donor. Indeed, the ATPγS reaction proceeded approximately 10-fold faster than the γ^{32}P-ATP reaction, again consistent with a dissociative reaction mechanism (Figure 7B). Because these reactions were carried out with magnesium as the sole divalent cation, a requirement for soft-metal−soft-ligand interactions (such as Mn−S) can be ruled out. The magnitude of the thio effect for the 2PTmin3.2-catalyzed reaction is consistent with the 2− 10-fold thio-effects observed on the spontaneous (uncatalyzed) hydrolysis of phosphate monoesters or diesters when the bridging oxygen is replaced by sulfur (*29−31*). In contrast, the 5′ phosphorylation reaction catalyzed by the Kin.46 ribozyme was approximately 50-fold faster with ATPγS than with γ^{32}P-ATP[24], suggesting that additional factors may influence reactivity for Kin.46.

DISCUSSION

We describe here a *trans*-acting ribozyme that phosphorylates exogenous RNAs containing the sequence **R**AAA-ANCG, where R in bold is the purine at the site of phosphorylation. Truncated variants of the selected isolates were generated based on secondary structural predictions. A minimized ribozyme was then separated into two strands that can assemble into an active complex through Watson−Crick base pairing. Alkaline digestion of chimeric DNA−RNA−DNA substrate strands before and after phosphoryl transfer mapped the phosphorylation site precisely to the 2′ hydroxyl group of G10$_S$. Mutational analysis on the substrate strand showed that this guanosine could be changed to an adenosine residue but that the four adenosines on the 3′ side of G10$_S$ were intolerant to mutation. These adenosines may form part of the active site structure, and they may help to position the 2′ OH or the ATP donor, or they may act through a combination of these effects.

The nearly flat pH−rate profile of the 2PTmin3.2 ribozyme over the range of pH 5.6 to 8.9, in combination with the approximately 10-fold thio effect in the presence of divalent magnesium, suggests that a step other than nucleophile activation or leaving group protonation is rate determining. This step could reflect some intrinsic feature of the chemistry of the γ-thiophosphoryl group—such as a dissociative, S_N1-like reaction mechanism—a required conformational change in the RNA, or another slow step. An intriguing alternative possibility is that the thiol effect results from differential binding interactions between the ribozyme and the ATPγS substrate vs its interactions with ATP. Given that our reactions are carried out at ATPγS concentrations (5 mM) that are 4-fold above K_m (1.3 mM), a 45-fold perturbation of K_m to approximately 60 mM would be required to achieve the observed 10-fold rate difference through K_m effects alone. This magnitude of a thiol effect on binding affinity would be unusual but not beyond possibility. Additional experimental information will be required to differentiate among these models.

Metal ions can assist ribozyme catalysis through a variety of mechanisms. They can stabilize secondary and tertiary structures through both diffuse and site-specific mechanisms, and they can neutralize backbone charge repulsion and the developing negative charges in nucleophiles, transition states, or leaving groups. Divalent ions can assist electrophilic catalysis by polarizing C−O or C−S bonds to increase the positive charge at the site of nucleophilic attack. They can orient ligands in their inner coordination sphere to interact with other active site species, and they can promote proton transfer by lowering the pK_a of bound water molecules (*26−29*). The present selection included seven divalents metal ions (Mg^{2+}, Ca^{2+}, Mn^{2+}, Co^{2+}, Cu^{2+}, Zn^{2+}, Ni^{2+}) and two monovalents cations (Na^+, K^+) to give the RNA population the opportunity to exploit the unique chemical properties of each ion (charge densities, Lewis acidities, preferred coordination geometries and bond lengths, dehydration energies, etc.). The reactivity of 2PTmin3.2 was strongly dependent on the total concentration of divalent ions but showed only a modest preference for specifications: $Mn^{2+} > Mg^{2+} > Ca^{2+}$. The lack of reactivity in the presence of cobalt hexamine suggested that these metal ions are making essential inner sphere contacts, perhaps with backbone phosphate or ribose oxygens. An alternative model would have the essential metal ion(s) participate in essential proton-transfer events, with the lack of reactivity in cobalt hexamine being due to disruption of these steps. The lack of pH dependence of the reaction seems to rule out this model.

A goal of this work was to evolve kinase ribozymes under conditions of competition for different regiospecificities. The selection permitted recovery of thiophosphoryl transfer onto one of the two hydroxyl groups of a tethered chloramphenicol or onto one of seven available 2′ hydroxyl groups near the 5′ end of the RNA chain. If we ignore the effects of the local environment, the pK_a of the Cam hydroxyls (10.2) is similar to that of a ribose 2′ hydroxyl (10.4); hence, their intrinsic reactivities (i.e., independent of catalyzed deprotonation) are likely to be similar. If the RNA population at the outset of the selection contained ribozymes of comparable activity targeted to each of the nine candidate sites at comparable frequencies, then two-ninths of the selected library should react at the tethered substrate. This line of thought predicts Cam reactivity for approximately 5 or 6 of the 24 sequences isolated. Instead, all isolates surveyed were fully reactive when transcribed as 126 nt RNAs without Cam. The isolates that were not assayed directly are very similar in sequence to those that were assayed, suggesting similar regiospecificity. We conclude that an incipient, evolving ribozyme population experiences an intrinsic predilection toward reacting with internal 2′ sites rather than with tethered substrates. As described below, such a predilection could be rooted in the mechanistic requirements for phosphoryl transfer catalysis.

Kinase ribozymes face the same two fundamental chemical challenges as those faced by protein enzymes: (i) positioning the substrate for in-line displacement, and (ii) promoting the exchange of bonds from donor to acceptor. For example, for phosphoglucomutase (PGM) to convert glucose-1-phosphate (Glc-1-P) into Glc-6-P, an enzyme-bound aspartyl phosphate is first transferred onto the 6- position of Glc-1-P to generate 1,6-bisphosphoglucose (1,6-BPG). This step utilizes a nondiffusible donor (phosphoenzyme) and a diffusible acceptor (Glu-1-P). The 1,6-BPG is then flipped over in the active site and the phosphoryl group on the 1-position is transferred back to the active site Asp. This step utilizes a diffusible donor (1,6-BPG) and a nondiffusible acceptor (enzyme Asp). To achieve specific positioning, the 1,6-BPG is held in the active site through a network of more than 20 hydrogen bonds, whereas only a few hydrogen bonds orient the nondiffusible Asp.

The reactions catalyzed by self-kinasing ribozymes are analogous to the second step catalyzed by PGM, utilizing a diffusible donor (ATP or other (d)NTP) and a nondiffusible acceptor (internal 2′ OH, terminal 5′ OH or tethered substrate). The fact that ribozyme 2PTmin3.2 exhibits saturation kinetics ($K_m^{\text{ATP}\gamma\text{S}} \approx 1.2$ mM) suggests that it may use its own network of interactions to stabilize its diffusible donor within its active site. In general, the structural complexity required to establish a network of interactions to position a given substrate within an active site is expected to correlate directly with the probability of encountering through selection catalysts that utilize that substrate. The nine potential acceptors (two Cam hydroxyls and seven ribose 2′ hydroxyls) are all present at high local concentration, but they must nevertheless be held in a productive orientation for in-line displacement. The conformation of the sugar—phosphate backbone is necessarily more constrained than that of the more mobile tethered Cam substrate. The Cam moiety therefore acts as a "quasi-diffusible," rather than a "nondiffusible" substrate. Constructing a binding site to orient the Cam moiety may require the specification of a greater number of nucleotides to form a more complex structure than one that orients a ribose hydroxyl.

Several groups have reported the selection of ribozymes that modify quasi-diffusible tethered substrates (*5, 32−34*). However, in many of these selections (e.g., ribozymes for Diels−Alder and Michael condensations), experimental design ensured only one possible site of reaction. The work present here is therefore unique in offering competition between approximately equivalent sites. Ribozymes that phosphorylate internal 2′ hydroxyls were identified by Lorsch and Szostak and were found to have k_{cat} and K_m values that are 5−10-fold improved relative to those of 2PT3.2; however, the numerous differences in experimental design preclude a quantitative comparison of the two sets of ribozymes, such as the inclusion by those authors of mutagenic cycles of amplification, selection steps that utilized significantly lower ATPγS concentrations (0.1 mM), and shorter incubation times (3 min) than those utilized here, and the lack of any constraints on the locations of the phosphoryl modification (*9*). Given an appropriate partition scheme that enforces regiospecificity, we do not foresee any insurmountable barrier to the identification of rapid, efficient ribozymes that phosphorylate Cam. Indeed, we have recently

developed such a scheme to be described elsewhere (Saran, D., Burke, D. H., manuscript in preparation). However, if ribozymes can be generated through selections to phosphorylate Cam or other tethered substrates, their increased complexity can be expected to make them more rare in the starting library than ribozymes with 2′-phosphotransferase (2PT) activity, even when only a small number of the ribose hydroxyls are permitted to react with the ATPγS. By extension, some of the metabolic ribozymes used during the postulated "RNA world" may have evolved incrementally through stages, arising first as self-modifying species that acted upon nondiffusible (backbone) or quasi-diffusible (tethered) substrates, with recognition of fully diffusible substrate appearing as subsequent refinement.

SUPPORTING INFORMATION AVAILABLE

This material is available free of charge via the Internet at http://pubs.acs.org.

REFERENCES

1. Bartel, D. P., and Szostak, J. W. (1993) Isolation of new ribozymes from a large pool of random sequences, *Science 261*, 1411−1418.
2. Ekland, E. H., and Bartel, D. P. (1996) RNA-catalysed RNA polymerization using nucleoside triphosphates, *Nature 382*, 373−376.
3. Illangasekare, M., Sanchez, G., Nickles, T., and Yarus, M. (1995) Aminoacyl-RNA synthesis catalyzed by an RNA, *Science 267*, 643−647.
4. Wiegand, T. W., Janssen, R. C., and Eaton, B. E. (1997) Selection of RNA amide synthases, *Chem. Biol. 4*, 675−683.
5. Tarasow, T. M., Tarasow, S. L., and Eaton, B. E. (1997) RNA-catalysed carbon−carbon bond formation, *Nature 389*, 54−57.
6. Wilson, C., and Szostak, J. W. (1995) In vitro evolution of a self-alkylating ribozyme, *Nature 374*, 777−782.
7. Lohse, P. A., and Szostak, J. W. (1996) Ribozyme-catalysed amino acid transfer reactions, *Nature 381*, 442−444.
8. Sheppard, T. L., Ordoukhanian, P., and Joyce, G. F. (2000) A DNA enzyme with N-glycosylase activity, *Proc. Natl. Acad. Sci. U.S.A. 97*, 7802−7807.
9. Lorsch, J. R., and Szostak, J. W. (1994) In vitro evolution of new ribozymes with polynucleotide kinase activity, *Nature 371*, 31−36.
10. Burke, D. H. (2004) Ribozyme-Catalyze Genetics, in *The Genetic Code and the Origin of Life* (Ribas de Pouplana, L., Ed.) p 48−74, Kluwer Academic/Plenum Publishers, Norwell, MA.
11. Li, Y., and Breaker, R. R. (1999) Phosphorylating DNA with DNA, *Proc. Natl. Acad. Sci. U.S.A. 96*, 2746−2751.
12. Greer, C. L., Peebles, C. L., Gegenheimer, P., and Abelson, J. (1983) Mechanism of action of a yeast RNA ligase in transfer-RNA splicing, *Cell 32*, 537−546.
13. Konarska, M., Filipowicz, W., Domdey, H., and Gross, H. J. (1981) Formation of a 2′-phosphomonoester, 3′,5′-phosphodiester linkage by a novel RNA ligase in wheat-germ, *Nature 293*, 112−116.
14. Konarska, M., Filipowicz, W., and Gross, H. J. (1982) RNA ligation via 2′-phosphomonoester, 3′,5′-phosphodiester linkage − requirement of 2′,3′-cyclic phosphate termini and involvement of a 5′-hydroxyl polynucleotide kinase, *Proc. Natl. Acad. Sci. U.S.A. 79*, 1474−1478.
15. Sekine, M., Iimura, S., and Furusawa, K. (1993) synthesis of a new class of 2′-phosphorylated oligoribonucleotides capable of conversion to oligoribonucleotides. *J. Org. Chem. 58*, 3204−3208.
16. Tsuruoka, H., Shohda, K., Wada, T., and Sekine, M. (2000) Synthesis and conformational properties of oligonucleotides incorporating 2′-O-phosphorylated ribonucleotides as structural motifs of pre-tRNA splicing intermediates, *J. Org. Chem. 65*, 7479−7494.

17. Rhee, S. S., and Burke, D. H. (2004) Tris(2-carboxyethyl)-phosphine stabilization of RNA: comparison with dithiothreitol for use with nucleic acid and thiophosphoryl chemistry, *Anal. Biochem. 325*, 137−143.

18. Igloi, G. L. (1988) Interaction of transfer-RNAs and of phospho-rothioate-substituted nucleic-acids with an organomercurial − probing the chemical environment of thiolated residues by affinity electrophoresis, *Biochemistry 27*, 3842−3849.

19. Santoro, S. W., and Joyce, G. F. (1997) A general purpose RNA-cleaving DNA enzyme, *Proc. Natl. Acad. Sci. U.S.A. 94*, 4262−4266.

20. Hati, S., Boles, A. R., Zaborske, J. M., Bergman, B., Posto, A. L., and Burke, D. H. (2003) Nickel(2+)-mediated assembly of an RNA-amino acid complex, *Chem. Biol. 10*, 1129−1137.

21. Breaker, R. R., Emilsson, G. M., Lazarev, D., Nakamura, S., Puskarz, I. J., Roth, A., and Sudarsan, N. (2003) A common speed limit for RNA-cleaving ribozymes and deoxyribozymes, *RNA 9*, 949−957.

22. Herschlag, D., and Jencks, W. P. (1989) Evidence that meta-phosphate monoanion is not an intermediate in solvolysis reactions in aqueous-solution, *J. Am. Chem. Soc. 111*, 7579−7586.

23. Herschlag, D., and Jencks, W. P. (1990) Catalysis of the hydrolysis of phosphorylated pyridines by Mg(OH)$^+$ − A possible model for enzymatic phosphoryl transfer, *Biochemistry 29*, 5172−5179.

24. Cleland, W. W., and Hengge, A. C. (1995) Mechanisms of phosphoryl and acyl transfer, *FASEB J. 9*, 1585−1594.

25. Tremblay, L. W., Zhang, G. F., Dai, J. Y., Dunaway-Mariano, D., and Allen, K. N. (2005) Chemical confirmation of a pentava-lent phosphorane in complex with beta-phosphoglucomutase, *J. Am. Chem. Soc. 127*, 5298−5299.

26. Lahiri, S. D., Zhang, G. F., Dunaway-Mariano, D., and Allen, K. N. (2003) The pentacovalent phosphorus intermediate of a phosphoryl transfer reaction, *Science 299*, 2067−2071.

27. Knowles, J. (2003) Chemistry: Seeing is believing, *Science 299*, 2002−2003.

28. Allen, K. N., and Dunaway-Mariano, D. (2003) Response to comment on The pentacovalent phosphorus intermediate of a phosphoryl transfer reaction, *Science 301,* 1184.

29. Breslow. R, and Katz, I. (1968) Relative reactivities of *p*-nitrophenyl phosphate and phosphorothioate toward alkaline phosphatase and in aqueous hydrolysis, *J. Am. Chem. Soc 90*, 7376−7377.

30. Domanico, P., Mizrahi, V., and Benkovic, S. J. (1986) *Mechanisms of Enzymatic Reactions: Stereochemistry*, *Proceedings of the 15th Steenbock Symposium* (Frey, P., Ed.) pp 127−138, University of Wisconsin-Madison, June 30−July 3, 1985, Elsevier, New York.

31. Herschlag, D., Piccirilli, J. A., and Cech, T. R. (1991) Ribozyme-catalyzed and nonenzymatic reactions of phosphate diesters − rate effects upon substitution of sulfur for a nonbridging phosphoryl oxygen atom, *Biochemistry 30*, 4844−4854.

32. Sengle, G., Eisenfuhr, A., Arora, P. S., Nowick, J. S., and Famulok, M. (2001) Novel RNA catalysts for the Michael reaction, *Chem. Biol. 8*, 459−473.

33. Coleman, T. M., and Huang, F. Q. (2002) RNA-catalyzed thioester synthesis, *Chem. Biol. 9*, 1227−1236.

34. Zhang, B. L., and Cech, T. R. (1997) Peptide bond formation by in vitro selected ribozymes, *Nature 390*, 96−100.